Published in final edited form as:

Biochemistry. 2006 March 14; 45(10): 3325–3336. doi:10.1021/bi0515927.

Chondrocytes Utilize a Cholesterol-Dependent Lipid Translocator To Externalize Phosphatidylserine[†]

Monika Damek-Poprawa[‡], **Ellis Golub**[‡], **Linda Otis**[§], **Gerald Harrison**[‡], **Christine Phillips**[‡], and **Kathleen Boesze-Battaglia**[*,‡]

[‡]Department of Biochemistry, University of Pennsylvania School of Dental Medicine, Philadelphia, Pennsylvania 19104

[§]Department of Diagnostic Sciences and Pathology, University of Maryland, Baltimore, Maryland 21201

Abstract

During endochondral ossification, growth plate chondrocytes release plasma membrane (PM) derived matrix vesicles (MV), which are the site of initial hydroxyapatite crystal formation. MV constituents which facilitate the mineralization process include the integral membrane ectoenzymes alkaline phosphatase (ALPase) and nucleotide pyrophosphatase phosphodiesterase (NPP1/PC-1), along with a phosphatidylserine- (PS-) rich membrane surface that binds annexins and calcium, resulting in enhanced calcium entry into MV. In this study, we determined that chick growth plate MV were highly enriched in membrane raft microdomains containing high levels of cholesterol, glycophosphatidylinositol- (GPI-) anchored ALPase, and phosphatidylserine (PS) localized to the external leaflet of the bilayer. To determine how such membrane microdomains arise during chondrocyte maturation, we explored the role of PM cholesterol-dependent lipid assemblies in regulating the activities of lipid translocators involved in the externalization of PS. We first isolated and determined the composition of detergent-resistant membranes (DRMs) from chondrocyte PM. DRMs isolated from chondrocyte PM were enhanced in ganglioside 1 (GM1) and cholesterol as well as GPI-anchored ALPase. Furthermore, these membrane domains were enriched in PS (localized to the external leaflet of the bilayer) and had significantly higher ALPase activity than non-cholesterol-enriched domains. To understand the role of cholesterol-dependent lipid assemblies in the externalization of PS, we measured the activities of two lipid transporters involved in PS externalization, aminophospholipid translocase (APLT) and phospholipid scramblase (PLSCR1), during maturation of a murine chondrocytic cell line, N1511. In this report, we provide the first evidence that maturing chondrocytes express PLSCR1 and have scramblase activity. We propose that redistribution of PS is dependent on an increase in phospholipid scramblase activity and a decrease in APLT activity. Lastly, we show that translocator activity is most likely to be modulated by membrane cholesterol levels through a membrane raft microdomain.

[†]This work was supported by USPHS Grant DE13576.

[*]Address correspondence to this author. Phone: 215-898-9167. Fax: 215-898-3695. battagli@biochem.dental.upenn.edu.

Vertebrate skeletal growth occurs largely through a highly regulated process known as endochondral ossification. During this process mesenchymal cells condense and differentiate into chondrocytes to form a cartilage template. Chondrocytes proliferate and then undergo a complex maturation process associated with an increase in cell size (hypertrophy). This hypertrophic stage is characterized by upregulation of the expression of genes encoding ALPase,[1] type X collagen, and matrix metalloproteinase-13, followed by mineralization of the extracellular matrix. The zones of proliferating, prehypertrophic and hypertrophic chondrocytes form the growth plate cartilage that controls the longitudinal growth of endochondral bone (1).

In calcifying cartilage, ALPase containing MV bud from the cell membrane and are released into the matrix, where they are believed to form the initial site of mineral development (2–4). MV budding from chondrocyte membranes is believed to occur at localized areas with a distinctive membrane composition. This conclusion is supported by comparative lipid and protein studies of the MV and the PM of the epiphyseal chondrocytes; MV contain higher concentrations of acidic phospholipids [phosphatidylserine (PS) and phosphatidylinositol (PI)] than the chondrocyte PM, and MV contain fewer proteins than PM (5). Previous studies in our laboratories have shown that MV function depends on membrane-anchored ALPase and the ability of the PS-rich membrane surface to recruit annexins and to be permissive for annexin-mediated Ca^{2+} entry (5, 6). The latter activity is critically dependent on the presence of high levels of membrane PS. We have also shown that hypertrophic chondrocyte cultures can form vesicles which are very similar to MV formed in vivo (7). These investigations indicated subtle structural differences in the composition of the two membranes, suggesting that MV originate from specific sites on the chondrocyte plasma membrane through a rearrangement of membrane components.

Two key features of MV, therefore, are the high levels of ALPase activity and the externalization of PS. Both of these membrane-associated processes may arise from PM assemblies, which form during chondrocyte development. It is well documented that many plasma membranes consist of microscopically and biochemically distinguishable lipid microdomains, which form liquid-ordered phases in the lipid bilayer and are dispersed in the bulk of the liquid-disordered phase of the plasma membrane (8–14). Membrane bilayer organization into these microdomains, known colloquially as membrane rafts or lipid assemblies, provides the requisite temporal and spatial organization of protein and lipid components necessary for normal cellular function (15–18). A unique property of these membrane rafts is their resistance to solubilization by mild detergents such as Triton X-100 (at low temperature), NP-40, and Brij-98; this insolubility is due, in part, to long saturated acyl chains of sphingomyelin that impart a high degree of order and also by stabilization of intercalating cholesterol molecules (8, 19).

[1]Abbreviations: APLT, aminophophospholipid translocase; OG, octyl glucopyranoside; DRM, detergent-resistant membrane; PS, phosphatidylserine; ALPase, alkaline phosphatase; PG, phosphatidylglycerol; PC, phosphatidylcholine; PE, phosphatidylethanolamine; PS, phosphatidylserine; PA, phosphatidic acid; PI, soy phosphatidylinositol; RBCs, red blood cells; NBD-PS, 1-oleoyl-2-[6-[(7-nitro-2,1,3-benzoxadiazol-4-yl)amino]caproyl]-*sn*-glycero-3-phosphoserine; NBD-PC, 1-oleoyl-2-[6-[(7-nitro-2,1,3-benzoxadiazol-4-yl)amino]caproyl]-*sn*-glycero-3-phosphocholine.

In addition to their unique lipid profile, membrane rafts also contain a number of proteins involved in signal transduction, thereby providing a signaling platform that enhances signal efficiency and specificity. The organization of these assemblies restricts access so that only a limited class of membrane proteins resides in rafts; these include proteins attached to the membrane by a lipid anchor, such as glycosylphosphatidylinoisitol- (GPI-) anchored proteins, acylated cytosolic proteins, and certain transmembrane proteins (15, 16, 20–22). Membrane rafts are involved in cellular processes as diverse as fertilization, viral infection, maintenance of cell polarity, chemotaxis, apoptosis, and development (15, 16, 22–28). Processes which involve changes in the shape of the cell, including domain-induced budding and possibly MV formation, are associated with membrane microdomains (29–34). On the basis of our studies, we propose that a reorganization of cholesterol-dependent lipid assemblies; i.e., lipid rafts, is a prerequisite for chondrocyte hypertrophy, an event considered critical for cartilage mineralization.

The phospholipid composition of the chondrocyte membrane is also crucial for function. PS is linked to the recruitment of annexin V which functions as a Ca^{2+} channel (6, 35). Annexin binding requires a charged PS-rich cytoplasmic membrane leaflet and the maintenance of normal lipid asymmetry. PS asymmetry is maintained by at least two lipid translocators, the calcium-independent, aminophospholipid translocase (APLT), involved in actively transporting PS from the outer to the inner monolayer, and the calcium-dependent phospholipid scramblase (36–38). Apoptotic cells, including terminally differentiated chondrocytes, exhibit an externalization of PS which is accompanied by both a loss of APLT activity and an increase in phospholipid scramblase activity (36, 39–42). In the experiments described below we show that (i) chondrocytes express phospholipid scramblase 1 (PLSCR1), (ii) PLSCR1 expression appears to be upregulated in BMP/Ins-treated cells, (iii) scramblase activity increases and amino phospholipid translocase activity decreases in early chondrocyte hypertrophy resulting in the externalization of PS, and (iv) these lipid translocator activities are dependent on membrane cholesterol levels.

MATERIALS AND METHODS

Release of Chicken Epiphyseal Growth Plate Chondrocytes and MV

Growth plate cartilage harvested from 8–10-week-old chicken tibia was minced and initially incubated (16 h at 4 °C) in digestion medium consisting of Hank's balanced salts solution (HBSS; Sigma, St. Louis, MO) containing bacterial collagenase (0.5%; Worthington) and hyaluronidase (7.5 units/mL; Sigma) and incubated in fresh digestion medium for 3 h at 37 °C. The minced digested cartilage was washed with cold HBSS (twice) to remove residual enzyme activity. Chondrocytes and MV were released by repeated trituration (30–40 cycles) through a 10 mL glass pipet. The resultant slurry was passed through a 40 mesh stainless steel sieve, the retentate resuspended in HBSS, and trituration repeated until 120–130 mL of filtrate was accumulated. The filtrate was centrifuged for 5 min at 10000*g*. The supernate (S1) was used to isolate MV, while the pellet (P1) was used to prepare chondrocyte plasma membrane.

Isolation of Matrix Vesicles

Supernate S1 was clarified by centrifugation at 15000*g* for 15 min, and MV were collected by centrifugation at 140000*g* for 240 min. MV pellets were resuspended in TES-salt buffer (10 mM TES-HCl, pH 7.4, and 150 mM NaCl; TSB) and purified by isopycnic density gradient centrifugation on sucrose density gradients (0–65% sucrose, in TSB) centrifuged at 197000*g* for 20 h.

Isolation of Chondrocyte Plasma Membranes

Red blood cells (RBCs) were manually removed from the pellet fraction (P1), and the residual chondrocyte pellet was resuspended in HBSS and centrifuged at 10000*g* for 5 min. Any residual RBCs were lysed by resuspension of the chondrocyte pellet in 5 mL of distilled water. After 2 min tonicity was restored with the addition of an excess of HBSS (4-fold), and chondrocytes resedimented. The chondrocyte pellet was resuspended in 50–60 mL of HBSS, and debris was removed by passage of the suspension sequentially through cheesecloth. The purified chondrocytes were subsequently sedimented and resuspended in TSB. Cells were lysed by rapid passage through an 18 gauge needle to maximize cell breakage and minimize organelle damage (43). Plasma membranes (PM) were isolated by isopycnic gradient centrifugation as described above. The purified MV and chondrocyte membrane preparations were analyzed for the RBC plasma membrane marker glycophorin-C (44). Our analysis showed no detectable glycophorin from contaminating RBC membrane as determined by Western blot analysis (data not shown). This analysis was expected to detect as little as 1 pg of glycophorin/20 μg of membrane protein. In addition, the cell suspensions, corresponding to 5×10^5 chondrocytes/mL, contained no detectable heme based on spectrophometric analysis at 420 nm (data not shown). This analysis allows us to detect as little as 10 pg of heme/mL of cell suspension, which corresponds to 0.333 RBC/mL.

Isolation of Triton X-100 Resistant Membrane Rafts

Triton X-100 resistant membrane rafts were prepared from chick chondrocyte PM and chick matrix vesicles essentially as described previously for photoreceptors (45). Briefly, purified chondrocyte PM or MV were washed, and the pellet was resuspended in 1 mL of MOPS buffer. Triton X-100 (2% w/v) was added to the cell suspension to yield a final concentration of 1% Triton X-100; this corresponds to 0.77 mL of 2% Triton X-100. To distinguish between Triton X-100 resistant membranes and nonraft partial detergent dependent solubilization, control cells were homogenized in 2% octyl glucopyranoside (OG) in parallel with Triton X-100 treated samples. Both Triton X-100 and OG treated samples were homogenized with three passes of a glass pestle through a glass Tenboeck tissue grinder. The detergent homogenate was mixed with 1.24 mL of 2.4 M sucrose to yield a final sucrose concentration of 0.9 M, transferred to a SW 41 centrifuge tube, overlayed with 1.0 mL of 0.8, 0.70, 0.65, 0.60, 0.55, and 0.50 M sucrose, and centrifuged at 40000 rpm for 20 h at 4 °C.

Analysis of Lipid Composition

Cholesterol (46) and total phosphate (47) were determined by standard procedures. Lipids were extracted from the low buoyant density fraction by a modification of the procedure of Bligh and Dyer (48); prior to the extraction of lipids from the detergent-solublized fractions, these samples were dialyzed for 48 h against two changes of 10 mM Hepes and 0.5 M NaCl, pH 7.4, to decrease the detergent concentration (49). In both PM and MV preparations, 90 ± 3.6% of the total phospholipid was extracted, indicating that the presence of residue detergent (Triton X-100 or OG) in the solublized fractions did not interfere with the extraction. Chloroform extracts were evaporated under nitrogen and diluted into chloroform immediately prior to lipid analysis by gradient elution using normal phase HPLC/ELSD (Avanti-Polar Lipids, Alabaster, AL). Standards (1 mg/mL) included triolein, cholesterol, ceramide, oleic acid, phosphatidylglycerol (PG), phosphatidylcholine (PC), phosphatidylethanolamine (PE), phosphatidylserine (PS), phosphatidic acid (PA), and soy phosphatidylinositol (PI). Standards and samples were injected on a normal phase HPLC column and analyzed by an evaporative light scattering detector (ELSD). A five-level calibration curve was used to calculate the amount of lipid species in each sample. In addition, chloroform extracts were analyzed by sequential thin-layer chromatography. The lipids were resolved on silica gel H plates developed in chloroform/methanol/acetic acid/water (25:15:4:2). The plates were developed in the same solvent system three times (50). Spots were identified by comparison to the migration patterns of known standards following staining with Dragendorf, ninhydrin, and sulfuric acid charring. The spots were scraped, and total phosphate was determined (47).

Ganglioside 1 (GM1) in the detergent-resistant and soluble fractions was detected by spotting 1 μL of sample directly onto nitrocellulose membranes. Membranes were blocked in BLOTTO, incubated at 21 °C with the β-subunit of cholera toxin (CtB; 85 ng/mL; Sigma) for 12 h, washed and exposed to anti-CTB conjugated to horseradish peroxidase, and analyzed by digital densitometry (Kodak Image Systems). Samples were adjusted for phosphate content.

N1511 Cell Culture and Induction with BMP-2/Insulin in Serum-Free Media

N1511 cells (51) (obtained from Dr. M. Iwamoto and Dr. V. Srinivas, Thomas Jefferson University, Philadelphia, PA) were plated at a high density (1.7×10^6 cells per well) in six-well plates and cultured in α-minimum essential media (α-MEM) supplemented with 10% FBS and 1% penicillin/streptomycin at 37 °C in 5% CO_2 (all reagents were from Sigma-Aldrich Co., St. Louis, MO). After 24 h the culture medium was changed to 0.3% FCS media, and the cells were induced with 50 ng/mL recombinant human BMP-2 (R&D Systems, Minneapolis, MN) and 1×10^{-6} M bovine insulin (Life Technologies, Inc., Grand Island, NY). L-Ascorbic acid phosphate magnesium salt (50 μg/mL; Wako Pure Chemical Industries, Ltd.) was also added directly into each well. Untreated cells in complete media constituted a control. The medium was changed every other day. On the third, fifth, seventh, and tenth day of treatment, total RNA was harvested from one set of cells, and the other set was stained for alkaline phosphatase.

During differentiation, prechondrocytes cease producing type I collagen and express cartilage-specific extracellular matrix genes encoding aggrecan and cartilage-specific collagens such as type II. Upon hypertrophy, they express type X collagen and upregulate ALPase. Within 72 h of BMP/Ins treatment, aggrecan mRNA had appeared, and Col II had decreased (data not shown). Extracellular MV were observed within 20 days (data not shown).

Laser Confocal Microscopy

N1511 cells were plated at a high density of 1.7×10^6 cells per Delta TPG 0.17 mm (black) dish (Fisher Scientific) and cultured in α-minimum essential media supplemented with 10% fetal calf serum and 1% penicillin/streptomycin at 37 °C in 5% CO_2 (all reagents were from Sigma-Aldrich Co.). After 24 h the cells were induced with 50 ng/mL recombinant human BMP-2 (R&D Systems), 1×10^{-6} M bovine insulin (Life Technologies, Inc.), and 50 μg/mL L-ascorbic acid phosphate (Wako) in media containing 0.3% FCS. The media were changed every other day. On the given day of treatment the cells were stained with 7 μg/mL cholera toxin conjugated to AlexaFluor 594 (Molecular Probes) (shown in red) to label GM1. GM1 was cross-linked with 40 μg/mL (1:25 dilution) anti-cholera toxin (Calbiochem) before fixation of cells with 2% paraformaldehyde. The cells were co-stained with 5 μg/mL rabbit anti-PLSCR Ab-1 (Oncogene) and subsequently incubated with goat anti-rabbit IgG AlexaFluor 488 secondary antibody at a concentration of 8 μg/mL (Molecular Probes) (shown in green). The fluorescent dye 4′,6′-diamidino-2-phenylindole (DAPI; Sigma) was used to visualize nuclei (shown in blue). Images of cells were taken on a Bio-Rad Radiance 2100 confocal microscope (Bio-Rad, Hercules, CA) using a 60× objective. DAPI, AlexaFluor 488, and AlexaFluor 594 fluorescence was excited by blue diode, argon (488 nm), and red diode lasers, respectively. Fluorescence emission was captured using the following filters: 376 ± 24 nm (DAPI), 515 ± 30 nm (AlexaFluor 488), and above 600 nm (AlexaFluor 594). All images were captured with the same laser settings. Analysis of fluorescent probe colocalization was performed using image analysis software (Metamorph; Universal Imaging Corp., Downingtown, PA). Regions of interest were defined to include cells that did not overlap. The region was segmented to select pixels above a constant threshold value (>60% above background) which represent true fluorescence. Since both spatial location and intensity of pixels contribute to colocalization, the values represent the integrated intensity; pixels in both AlexaFluor 488 and AlexaFluor 594 images had similar brightness values and spatial location. Colocalization analysis was performed on all cells present in Figure 5.

RNA Isolation and Analysis

The cell layer was washed with PBS, and total RNA was isolated using TRI reagent (Molecular Research Center, Inc., Cincinnati, OH). RNA yield was determined by absorbance at 260 nm and integrity confirmed by gel electrophoresis. Total RNA (5 μg) was converted into cDNA using the SuperScript first-strand synthesis system for RT-PCR (Invitrogen, Carlsbad, CA). The cDNA samples were amplified in a Smart Cycler (Cepheid, Inc., Sunnyvale, CA) with LightCycler Fast-Start DNA Master SYBR Green I reagent (Roche Molecular Biochemicals, Mannheim, Germany) using specific primers. Gene expression was normalized using GAPDH primers. Specific primers for collagen X and

PLSCR1 were designed as follows: Col X, (F) cgtgtctgcttttactgtca, (R) acctggtcattttctgtgag; PLSCR1, (F) tagctgctgttccgacattg, (R) tgctcctcgtttccagttct. The results from real-time RT-PCR were obtained as crossing points, indicating the number of cycles required for fluorescence of the PCR product to increase above threshold value. These crossing points were converted to arbitrary units of mRNA assuming a concentration-dependent straight line for a semilog plot, with a value of 3.5 for the fold change in mRNA/cycle (slope), and the crossing point cycle number with no template as an estimate of the *y*-intercept (52, 53). A final melt curve from 60 to 95 °C was performed to confirm the specificity of the PCR, and the identities of PCR products were checked by gel electrophoresis.

Alkaline Phosphatase Activity and Staining

Alkaline phosphatase activity was assayed in a reaction mixture containing *p*-nitrophenyl phosphate (5 mM) in Tris-HCl buffer (1.5 M, pH 9.0) supplemented with $ZnCl_2$ (1.0 mM) and $MgCl_2$ (1.0 mM). Enzyme activity was monitored by following the production of *p*-nitrophenol at 410 nm in a recording spectrophotometer. Rates were expressed as micromoles of *p*-nitrophenol per minute per milligram of protein (in membrane raft preparations) and nanomoles of *p*-nitrophenol per minute per 1×10^6 cells in N1511 experiments. In both cases, a value of 16.0 was used for the millimolar extinction coefficient. Protein assays were performed using the Micro BCA protein assay reagent kit (Pierce, Rockford, IL). For alkaline phosphatase staining, cell monolayers were washed twice with TBS, fixed in 2% paraformaldehyde in methanol for 1 min at 4 °C, and stained with naphthol AS-BI (Sigma).

Phospholipid Uptake

Aminophospholipid translocase (APLT) and phospholipid scramblase activities were measured using a well-characterized fluorescent lipid-uptake assay as described (36, 54, 55). APLT activity was determined by the uptake of 1-oleoyl-2-[6-[(7-nitro-2,1,3-benzoxadiazol-4-yl)amino]caproyl]-*sn*-glycero-3-phosphoserine (NBD-PS), and scramblase activity was determined by the uptake of 1-palmitoyl-2-[6-[(7-nitro-2,1,3-benzoxadiazol-4-yl)amino]-caproyl]-*sn*-3-glycerophosphocholine (NBD-PC). Briefly, treated cells (1×10^6) were washed and resuspended in 100 μL of Hepes-buffered saline (HBS) (137 mM NaCl, 2.7 mM KCl, 2 mM $MgCl_2$, 5 mM glucose, 10 mM Hepes, pH 7.4). Cells were incubated with 1 μL of NBD-lipid (50 μg/mL) at 37 °C for 30 min. Following incubation, cells were washed with 50 μL of 1% BSA to remove unincorporated probe lipid. Cells were subsequently labeled with 1 μL of propidium iodide (250 μg/mL) for 10 min. Samples were transferred to ice, diluted with 900 μL of HBS, and analyzed within 1 h on a Becton-Dickinson Facstar^{PLUS} flow cytometer (BD Biosciences, San Jose, CA). The mean fluorescence values of phospholipid uptake were determined by gating on viable (propidium iodide negative) cells. NBD and propidium iodide fluorescence was excited using an argon laser at 488 nm and fluorescence measured with a 530/30 nm and 630/22 nm band-pass filter, respectively. Fluorescence was detected using log amplification; a minimum of 10000 events were collected on each sample.

PS Externalization

Acyl-chain-labeled NBD-PS was incorporated into N1511 cells (1×10^6 cells/mL) as described above. All fluorescence measurements were performed on a Perkin-Elmer LS55B spectrofluorometer. Prior to the start of each experiment, $CaCl_2$ was added to the cell suspensions to a final concentration of 1 μM, and cells were transferred to cuvettes placed in a water- jacketed turret at 37 °C. Fluorescence of NBD-lipids was measured with excitation at 470 nm and emission at 525 nm. NBD-PS distribution was measured using a dithionite quenching assay as described (56). Briefly, the initial fluorescence (designated F_0) of the sample was recorded; 30 μL of 1 M dithionite was then added, and the fluorescence decrease was followed over time (usually 120 s) as the NBD probe in the outer monolayer was quenched. The addition of twice the amount of dithionite resulted in no additional quenching within the short 2 min incubation time. The fluorescence value F_r was recorded after the reaction was complete and the fluorescence had remained unchanged for 10 s. The addition of Triton X-100 caused a further decrease in fluorescence, such that essentially all of the remaining fluorescence was destroyed. When Triton X-100 was added prior to dithionite treatment, the addition of dithionite resulted in the quenching of 100% of the NBD fluorescence. Fluorescence values were corrected for the background fluorescence of unlabeled cells (designated F_{app}), which did not change over the course of the experiments. The amount of NBD-lipid accessible to dithionite was calculated from the decrease in cell-associated fluorescence after quenching with dithionite using the formula:

$$\% \text{ accessible} = \{1 - [(F_r - F_{app})/(F_0 - F_{app})]\} \times 100$$

Statistical Analyses

All data were analyzed using Sigma Stat software, Version 3.1, as described in the figure legends. The real-time RT-PCR samples were compared using a Tukey test in which P values below 0.050 were considered to show a statistically significant difference based on two-way ANOVA analysis. ANOVA on ranks was performed in order to test differences over time in the scramblase activity measured using flow cytometry. For the remaining cases one-way ANOVA was used for testing the differences in the lipid translocator activity.

RESULTS

Isolation of Triton X-100 Resistant Chondrocyte and Matrix Vesicle Fractions

Cartilage mineralization requires the formation of membrane buds termed matrix vesicles, which are enriched in ALPase, annexins II, V, and VII, and that associate with collagen types II and X. A number of these proteins require association with the membrane surface: ALPase through a GPI-linked anchor and annexin with PS-rich microdomains. Chondrocyte and MV-specific membrane microdomains were isolated by exploiting the relative insolubility of cholesterol-enriched membrane microdomains in detergent. Chondrocyte detergent-resistant membranes (DRMs) were isolated as a low buoyant density opaque band observed at a refractive index of 1.362, equal to 19% sucrose. Triton X-100 treated matrix vesicles showed a similar banding pattern with a low buoyant density band isolated at a RI = 1.3565, equal to 15.5% sucrose. The detergent-soluble fractions were isolated at 35%

sucrose. To account for nonspecific partial detergent solubilization of the membrane, samples were also lysed in 1% octyl glucopyranoside as a control.

The lipid composition of DRMs was analyzed for the membrane raft markers cholesterol, sphingomyelin, and GM1. As shown in Figure 1A,B, cholesterol accounts for approximately 50% of the total lipid in both chondrocyte (Figure 1A) and MV (Figure 1B) DRMs. Although sphingomyelin accounted for less than 10% of the total lipid in both chondrocyte membrane preparations and MV, it was enhanced in both chondrocyte and MV DRMs (Figure 1A,B). In addition, both chondrocyte and MV DRMs were enriched in GM1 (Table 1). To determine what proportion of the membrane phospholipid was resistant to detergent extraction, phosphate levels in DRMs were compared to those in the detergent-soluble fractions. Interestingly, chondrocyte DRMs comprised 6.9% of the total membrane phospholipid, while MV rafts comprised over 32% of the total phospholipid (Table 1). Nonfractionated chondrocyte membranes had ALPase levels per milligram of protein that were one-fifth that of membrane rafts, and the ALPase specific activity in purified MV was only twice that in raft preparations (Table 2).

Although membrane assemblies are enriched in a number of lipids, the phospholipid profile of membrane microdomains varies considerably; for example, platelets contain PS-enriched membrane rafts (57, 58). Since chondrocyte mineralization requires PS, we investigated the phospholipid profile of MV and chondrocyte DRMs (Figure 1C,D). Phosphatidylcholine content varied little between the detergent-soluble and detergent-insoluble membrane fractions. As expected, little phosphatidylethanolamine (a nonraft phospholipid) was detected in either chondrocyte or MV raft fractions. The most striking change in phospholipid content was observed with PS. In chondrocyte membrane preparations, detergent-soluble PS makes up 21% of the total lipid while in chondrocyte DRMs this lipid accounts for over 44% of the phospholipid (Figure 1C); in matrix vesicles (Figure 1D), PS accounts for less than 20% of the total detergent-soluble lipid and over 30% of the MV DRMs. Phosphatidylinositol, a raft-associated signaling lipid, comprises almost 10% of the chondrocyte raft and 5% of MV rafts. Collectively, these results suggest that both chondrocyte and MV DRMs have lipid profiles consistent with membrane rafts (and will hereafter be referred to as such).

We further investigated the transbilayer distribution of PS in the membrane using a fluorescence-quenching assay. NBD-PS-labeled chondrocytes or MV were used to assess outer monolayer PS detected as fluorescent probe quenched with the addition of 1 M sodium dithionite (56, 59). Chondrocyte DRMs isolated from the labeled membranes showed slightly higher levels of externalized PS than the parent chondrocyte membrane (92 ± 1.0% vs 86 ± 0.4%). Although present in much higher amounts, PS distribution in the MV appeared to be more similar to cell membrane, 79 ± 0.5% vs 76 ± 0.9%, in rafts and parent membrane, respectively. Collectively, these results suggest that the raft-associated PS in both membrane preparations is largely external.

Lipid Translocator Activities Change during Chondrocyte Maturation

Since both chondrocytes and MV rafts are enriched in PS, we hypothesized that the maintenance of PS asymmetry in chondrocytes may be a cholesterol-dependent event. Thus

we investigated the mechanism of PS translocation in maturing chondrocytes in a cartilage-derived clonal chondrocytic cell line: N1511 cells (51). N1511 cells were grown to confluence and treated with BMP-2 and insulin at day 1. During differentiation, chondrocyte precursors cease producing type I collagen and express cartilage-specific extracellular matrix genes encoding aggregan and cartilage-specific collagens such as type II. Upon hypertrophy, they express type X collagen. Consistent with studies by Kamiya et al. (51), we observed that uninduced N1511 cells at confluence showed little expression of Col X; by day 5, Col X expression had increased and stayed elevated (Figure 2A). The BMP-treated cells expressed higher levels of collagen X mRNA than corresponding control cells (*, $P < 0.001$ from the Tukey test). On day 10 the collagen X expression in the BMP-treated cells significantly increased as compared to days 3 and 7 (#, $P < 0.001$ from the Tukey test) and stayed elevated up through day 19 (data not shown). In uninduced control cells the collagen X mRNA level was the highest on day 7 as compared to day 3, 5, and 10 (**, $P < 0.01$ from the Tukey test).

Chondrocytes were analyzed for ALPase activity and cell surface staining at days 3, 5, 7, and 10. As shown in Figure 2B, BMP/Ins-treated N1511 cells show surface ALPase staining by day 3, with strong staining by days 7 and 10. We observed some variability in ALPase staining within the first 72 h postinduction, although in all experiments ALPase staining increased to the maximum by day 10. Throughout this same time period, ALP activity increased from 6.97 nmol of *p*-nitrophenyl phosphate/min per 1×10^6 cells at day 3 to 127 nmol of *p*-nitrophenyl phosphate/min per 1×10^6 cells at day 10 (Figure 2C). Untreated control cultures showed very few ALP-positive cells and no increase in ALPase activity.

Using this model system, we assessed PLSCR1 expression, lipid translocator activity, and PS distribution over the 10 day course of chondrocyte maturation, a time frame during which the cells underwent hypertrophy. PS redistribution is dependent on the relative activities of two lipid translocators, the aminophospholipid translocase (APLT) and the phospholipid scramblase (36, 60). Using real-time RT-PCR to analyze PLSCR1 mRNA levels, PLSCR1 expression in N1511 cells did not change over the course of 10 days, with or without BMP (Figure 3A). BMP/insulin-treated cells show higher levels of PLSCR1 expression than control cells [*, $P < 0.05$ compared with corresponding untreated (from the Tukey test)]. PLSCR1 appeared to localize to the plasma membrane in prehypertrophic (day 3) chondrocytes and a portion redistributed to the nucleus as the cells underwent late hypertrophy (Figure 3B). As shown in Figure 3C, PLSCR1 protein levels in maturing chondrocytes remained constant.

Lipid translocator activity was measured by following NBD fluorescent lipid uptake using flow cytometry (36, 41, 55). This well-characterized assay measures APLT activity as uptake of NBD-PS and scramblase activity as uptake of PC. Thus a decrease in APLT activity is manifest as little NBD-PS uptake and enhanced scramblase activity measured as an increase in NBD-PC uptake and the externalization of PS. N1511 cells isolated at days 3, 5, 7, and 10 were incubated with either acyl-chain-labeled NBD-PC or NBD-PS to measure scramblase and APLT activity, respectively. Representative cytometry histograms (Figure 4A) demonstrate APLT activity and scramblase activity. The activities of the translocators, determined as mean channel fluorescence (MCF), are quantitatively compared in Figure 4B

as percent of control activity. Upon BMP/Ins treatment, the N1511 cells showed a marked decrease in APLT activity and an initial increase in scramblase activity that began to diminish by day 7 (Figure 4B) and further decreased by day 10. The scramblase activity (solid bar) significantly increased at day 7 compared to day 3 ($P < 0.05$, from Dunn's test). At days 7 and 10 a significant decrease in APLT activity (open bar) was observed ($P < 0.01$, from the Student–Newman–Keuls method). Omission of calcium from the buffer resulted in no detectable outer leaflet PS and no change in scramblase activity (data not shown), consistent with Ca^{2+}-dependent scramblase activity observed in platelets and other cell types (61–65). To determine if the decreased APLT activity and increased scramblase activity resulted in the externalization of PS, the distribution of NBD-PS in the cells was measured using dithionite quenching techniques. As shown in Figure 4C, a 50% increase in the amount of PS externalized to the outer monolayer was observed by day 5, with no substantial increase observed after day 7, at which time over 80% of the PS had been externalized.

To determine if PLSCR1 localized to chondrocyte membrane rafts, N1511 cells isolated at various times, corresponding to stages of maturation, were first exposed to CtB–AlexaFluor 594 to identify GM1, and patches representing microdomains were induced by treatment with anti-CtB antisera (Figure 5B,E,H,K). Cells were then exposed to anti-PLSCR1 Ab for 2 h, washed, and stained with goat anti-rabbit IgG AlexaFluor 488 (Figure 5A,D,G,H). Analysis of merged images indicates that PLSCR1 is membrane raft associated in all samples; however, the relative levels of association decrease as the cells proceed through the late hypertrophic stage (Figure 5C,F,I,L). In the prehypertrophic stage virtually all PLSCR1 (>86%) fluorescence is found associated with the GM1 patches. In contrast, in hypertrophic and late hypertrophic stages only 35% and 10% of the PLSCR1 fluorescence was GM1 associated. Most intriguing is the observation that, during this same time period, 26% and 46% of the PLSCR1 fluorescence became associated with the nucleus; the implications of this redistribution are presently under investigation.

Since PLSCR1 appeared to be localized to membrane rafts, we determined if scramblase activity was cholesterol dependent. Scramblase activity was measured in chondrocytes treated with the cholesterol sequestrant, MβCD (66). Lipid translocator activities of N1511 cells isolated at days 3, 5, 7, and 10 were determined using flow cytometry as shown below in Figure 4A. These cells were immediately depleted of membrane cholesterol with 2 mM MβCD for 15 min as described (66). As shown in the cytometry histograms from FACS analysis (Figure 6A), cholesterol depletion with MβCD resulted in a net decrease in mean channel fluorescence in NBD-PC, indicating a decrease in scramblase activity. Data for both scramblase activity and APLT activity upon cholesterol depletion of BMP/insulin-treated chondrocytes are shown in Figure 6B. In the presence of MβCD, scramblase activity decreased and was the lowest at day 5 ($P < 0.001$, from the Student–Newman–Keuls method). Following MβCD addition, APLT activity at day 3 was significantly elevated as compared to the other time points. APLT activity was the lowest at day 7 ($P < 0.05$, from the Student–Newman–Keuls method). It should also be noted that the N1511 cells were not adversely affected by these agents; viability profiles of cells treated with MβCD were similar to control (untreated) cells (data not shown).

The association of cholesterol depletion with decreased scramblase activity is not unexpected since PLSCR1 has been shown to reside in cholesterol-enriched membrane rafts in myelomas, neutrophils, platelets, and RBCs (61, 64). Interestingly, by day 10, the effect of cholesterol depletion (i.e., membrane raft disruption) on scramblase activity was almost negligible, most likely due to the redistribution of PLSCR1 to the nucleus (Figure 3B, as seen previously (67). Collectively, these results suggest that PS externalization is dependent on the relative activities of scramblase and ALPT, most likely in a cholesterol-dependent manner.

DISCUSSION

In this study we provide the first evidence that membrane phosphatidylserine redistribution in chondrocytes occurs at an early stage in the maturation process, prior to late hypertrophy. On the basis of analysis of lipid translocator activities, we propose that the mechanism of externalization involves an increase in scramblase activity and a decrease in APLT activity. Cholesterol depletion studies suggest that these activities and by inference PS externalization are modulated by a decrease in membrane cholesterol.

It is well established that the process of chondrocyte maturation that is associated with MV formation requires an increase in the size of the chondrocyte and a change in shape of the chondrocyte membrane (2, 68, 69). Such changes in membrane architecture require both alterations within the membrane lipid components (either through altered synthesis or reorganization) and the regulated expression of matrix vesicle specific proteins. A reorganization of membrane components is commonly mediated by a redistribution of components within specialized membrane microdomains known as rafts. These are cholesterol- and GM1-enriched membrane domains that can be isolated as detergent-insoluble complexes. Utilizing detergent isolation techniques, we demonstrate that chondrocytes contain membrane raft domains comprising approximately 7% of the total membrane. It is noteworthy that when this same microdomain was isolated from MV, the lipid rafts comprised over 30% of the total membrane. During phase 1 of mineralization approximately this same percentage of membrane area (25–35%) is involved in the formation of intramembranous hydroxyapatite seed crystals (refs 2 and 3 and references cited therein). Moreover, the ALPase specific activity in isolated MV rafts was 10-fold higher than in rafts isolated from chondrocyte membranes. Whether this increased ALPase activity is due to higher levels of ALPase in these membranes or to a membrane-mediated effect on ALPase activity remains to be determined.

Rafts from chondrocyte membranes and matrix vesicles were also found to be enriched in PS, a lipid not commonly found at such high levels in these microdomains. The relative amount of PS is, however, comparable to the levels of PS observed in activated platelet rafts (57, 58, 70). In those membranes, PS is required for the formation of the prothrombinase complex. PS asymmetry is maintained by the relative activities of the lipid translocators, APLT and scramblase (36, 40, 60). Activities of these translocators are controlled by cytosolic calcium; when calcium levels exceed 1 mM, scramblase activity is enhanced and APLT activity decreases. In our studies, chelation of calcium with EDTA inhibited scramblase activity and blocked PS externalization (data not shown). Further, PS is believed

to play an important role in MV function by regulating annexin V calcium channel activity (6, 35). Thus, the high level of PS in rafts isolated from maturing chondrocytes supports the contention that raft formation in chondrocyte membranes is a precursor to and an integral part of MV biogenesis. The phospholipid composition of the MV rafts is somewhat unusual; although high in PS and cholesterol it is relatively low in sphingomyelin and PI. Given that the MV itself is a portion of specialized membrane which blebs from the parent chondrocyte membrane, its raft composition may be determined by its specialized function in mineralization.

Our identification of PLSCR1 is the first report that maturing chondrocytes express an isoform of this protein (71). PLSCR1 expression levels have been found to be altered in some cell types but not others, with levels directly correlated with stimulus-dependent movement of PS to the cell surface, thus suggesting that the PLSCR1 has scramblase activity (refs 36, 37, 41, and 42 and references cited therein). Although in our chondrocyte model the level of PLSCR1 expression appears to be constant over the 7 day maturation process, as is seen in neutrophils and some myeloma cells (61, 64), scramblase activity is altered in response to a decrease in chondrocyte membrane cholesterol. Lastly, PLSCR1 appears to localize to the plasma membrane by day 3 and subsequently redistribute to the nucleus by day 7, suggesting that it could be a multifunctional protein with both signaling properties and lipid translocator activity. The PLSCR1 gene is transciptionally activated by interferons and various growth factors (72, 73). PLSCR1 phosphorylation by cellular PKC γ promotes transbilayer redistribution of lipids in apoptotic cells (74). PLSCR1 also interacts directly with the β-secratase protein in amyloid plaque formation (75). Lastly, PLSCR1 is phosphorylated by c-Abl, and truncation of PLSCR1 is seen in a spontaneous murine mutation of this gene, which is linked to a leukemogenic transformation (76), although the precise role of PLSCR1 in the regulation of cell proliferation is unknown. Further studies are clearly needed to assess the dual function of PLSCR1 both in chondrocytes and in other systems.

Collectively, these results suggest that BMP/Ins induces PLSCR1 expression and that, upon chondrocyte hypertrophy, membrane rearrangement mediates scramblase-dependent PS cell surface exposure as a means to recruit and bind annexin in the mineralization process. Lastly, the nuclear localization of PLSCR1 in N1511 cells by day 7 of BMP/Ins treatment is similar to that observed in fibroblasts and suggests that PLSCR1 becomes depalmitoylated (67). The precise site of nuclear interaction is presently under investigation. PS has been shown both in vivo and in vitro to be required for annexin binding to the cytoplasmic surface of the chondrocyte to form a Ca^{2+} channel necessary for mineralization (6, 35). Interestingly, in those studies the authors concluded that binding of annexins to the membrane is not sufficient for channel formation and proposed that a specialized lipid component is required for annexin II, V, and VI to form Ca^{2+} channels. In more recent work, type II collagen has been shown to interact with annexin V (77). Our results suggest that the reorganization of the chondrocyte membrane during the prehypertrophic stage provides a specialized lipid domain, which is most likely cholesterol- and PS-enriched membrane rafts. We propose that this reorganization requires PS externalization, likely in a raft domain, and that this externalization may provide the driving force for the formation of

annexin channels in the membrane. The evidence in support of this hypothesis seems compelling: chondrocytes express PLSCR1 on the membrane surface, PS externalization in chondrocytes is shown to be due to a decrease in APLT activity and an increase in scramblase activity as chondrocytes undergo hypertrophy, and the activities of these lipid translocators are directly dependent on membrane cholesterol content. The role of membrane raft mediated proteins in mineralization is further supported by the observation that raft-associated annexin-2 is important in the osteoblastic mineralization process (78, 79), although those studies did not analyze cholesterol-dependent lipid translocators. Further studies in our laboratory designed to understand the molecular mechanism by which altered cholesterol biosynthesis and lipid redistribution contribute to MV formation are presently underway.

Acknowledgments

The authors thank Bruce J. Shenker and Phoebe S. Leboy for helpful insight and critical reading of the manuscript. We acknowledge the School of Dental Medicine Flow Cytometry and Imaging Facility for support of these studies.

References

1. Ballock RT, O'Keefe RJ. Physiology and pathophysiology of the growth plate. Birth Defects Res Part C. 2003; 69:123.
2. Anderson HC. Mechanism of mineral formation in bone. Lab Invest. 1989; 60:320. [PubMed: 2648065]
3. Anderson HC. Matrix vesicles and calcification. Curr Rheumatol Rep. 2003; 5:222. [PubMed: 12744815]
4. Schwartz Z, Amir D, Weinberg H, Sela J. Extracellular matrix vesicle distribution in primary mineralization two weeks after injury to rat tibial bone (ultrastructural tissue morphometry). Eur J Cell Biol. 1987; 45:97. [PubMed: 3443113]
5. Harrison G, Shapiro IM, Golub EE. The phosphatidylinositol-glycolipid anchor on alkaline phosphatase facilitates mineralization initiation in vitro. J Bone Mineral Res. 1995; 10:568.
6. Kirsch T, Nah HD, Demuth DR, Harrison G, Golub EE, Adams SL, Pacifici M. Annexin V-mediated calcium flux across membranes is dependent on the lipid composition: implications for cartilage mineralization. Biochemistry. 1997; 36:3359. [PubMed: 9116015]
7. Golub EE, Schattschneider SC, Berthold P, Burke A, Shapiro IM. Induction of chondrocyte vesiculation *in vitro*. J Biol Chem. 1983; 258:616. [PubMed: 6848521]
8. Simons K, Ikonen E. Functional rafts in cell membranes. Nature. 1997; 387:569. [PubMed: 9177342]
9. Simons K, Gruenberg J. Jamming the endosomal system: lipid rafts and lysosomal storage diseases. Trends Cell Biol. 2000; 10:459. [PubMed: 11050411]
10. Brown DA, London E. Functions of lipid rafts in biological membranes. Annu Rev Cell Dev Biol. 1998; 14:111. [PubMed: 9891780]
11. Brown RE. Sphingolipid organization in biomembranes: what physical studies of model membranes reveal. J Cell Sci. 1998; 111:1. [PubMed: 9394007]
12. Brown DA, London E. Structure and origin of ordered lipid domains in biological membranes. J Membr Biol. 1998; 164:103. [PubMed: 9662555]
13. Brown DA, London E. Structure and function of sphingolipid- and cholesterol-rich membrane rafts. J Biol Chem. 2000; 275:17221. [PubMed: 10770957]
14. Smart EJ, Graf GA, McNiven MA, Sessa WC, Engelman JA, Scherer PE, Okamoto T, Lisanti MP. Caveolins, liquid-ordered domains, and signal transduction. Mol Cell Biol. 1999; 19:7289. [PubMed: 10523618]
15. Pike LJ. Lipid rafts: bringing order to chaos. J Lipid Res. 2003; 44:655. [PubMed: 12562849]

16. Pike LJ. Lipid rafts: heterogeneity on the high seas. Biochem J. 2004; 378:281. [PubMed: 14662007]
17. van der Goot FG, Harder T. Raft membrane domains: from a liquid-ordered membrane phase to a site of pathogen attack. Semin Immunol. 2001; 13:89. [PubMed: 11308292]
18. Lipowsky R. Domains and rafts in membranes–Hidden dimensions of self-organization. J Biol Phys. 2002; 28:195. [PubMed: 23345769]
19. Claas C, Stipp CS, Hemler ME. Evaluation of prototype transmembrane 4 superfamily protein complexes and their relation to lipid rafts. J Biol Chem. 2001; 276:7974. [PubMed: 11113129]
20. Pizzo P, Viola A. Lymphocyte lipid rafts: structure and function. Curr Opin Immunol. 2003; 15:255. [PubMed: 12787749]
21. Perschl A, Lesley J, English N, Hyman R, Trowbridge IS. Transmembrane domain of CD44 is required for its detergent insolubility in fibroblasts. J Cell Sci. 1995; 108:1033. [PubMed: 7542666]
22. Moffett S, Brown DA, Linder ME. Lipid-dependent targeting of G proteins into rafts. J Biol Chem. 2000; 275:2191. [PubMed: 10636925]
23. Anderson RGW. Caveolae: Where incoming and outgoing messengers meet. Proc Natl Acad Sci USA. 1993; 90:10909. [PubMed: 8248193]
24. Anderson RGW. Plasmalemmal caveolae and GPI-anchored membrane proteins. Cell Biol. 1993; 5:647.
25. Anderson RGW. The caveolae membrane system. Annu Rev Biochem. 1998; 67:199. [PubMed: 9759488]
26. Mañes S, Mira E, Gómez-Moutón C, Lacalle RA, Keller P, Labrador JP, Martínez-A C. Membrane raft microdomains mediate front-rear polarity in migrating cells. EMBO J. 1999; 18:6211. [PubMed: 10562533]
27. Liu P, Anderson RG. Compartmentalized production of ceramide at the cell surface. J Biol Chem. 1995; 270:27179. [PubMed: 7592974]
28. van der Liu AH, Budde M, Ruurs P, Verheij M, van Blitterswijk WJ. Alkyl-lysophospholipid accumulates in lipid rafts and induces apoptosis via raft-independent endocytosis and inhibition of phosphotidylcholine synthesis. J Biol Chem. 2002; 277:38541.
29. Sabharanjak S, Sharma P, Parton RG, Mayor S. GPI-anchored proteins are delivered to recycling endosomes via a distinct cdc42-regulated, clathrin-independent pinocytic pathway. Dev Cell. 2002; 2:411. [PubMed: 11970892]
30. Sabharanjak S, Mayor S. Folate receptor endocytosis and trafficking. Adv Drug Delivery Rev. 2004; 56:1099.
31. Deckert M, Ticchioni M, Bernard A. Endocytosis of GPI-anchored proteins in human lymphocytes: role of glycolipid-based domains, actin cytoskeleton, and protein kinases. J Cell Biol. 1996; 133:791. [PubMed: 8666664]
32. Gomez-Mouton C, Abad JL, Mira E, Lacalle RA, Gallardo E, Jimenez-Baranda S, Illa I, Bernad A, Manes S, Martinez-A C. Segregation of leading-edge and uropod components into specific lipid rafts during T cell polarization. Proc Natl Acad Sci USA. 2001; 98:9642. [PubMed: 11493690]
33. Nichols BJ, Kenworthy AK, Polishchuk RS, Lodge R, Roberts TH, Hirschberg K, Phair RD, Lippincott-Schwartz J. Rapid cycling of lipid raft markers betweenthe cell surface and golgi complex. J Cell Biol. 2001; 153:529. [PubMed: 11331304]
34. Nichols BJ. Caveosomes and endocytosis of lipid rafts. J Cell Sci. 2003; 116:4707. [PubMed: 14600257]
35. Kirsch T, Harrison G, Golub E, Nah H. The roles of annexins and types II and X collagen in matrix vesicle-mediated mineralization of growth plate cartilage. J Biol Chem. 2000; 275:35577. [PubMed: 10956650]
36. Bratton DL, Fadok VA, Richter DA, Kailey JM, Guthrie LA, Henson PM. Appearance of phosphatidylserine on apoptotic cells requires calcium-mediated nonspecific flip-flop and is enhanced by loss of the aminophospholipid translocase. J Biol Chem. 1997; 272:26159. [PubMed: 9334182]
37. Daleke DL. Regulation of transbilayer plasma membrane phospholipid asymmetry. J Lipid Res. 2003; 44:233. [PubMed: 12576505]

38. Martin OC, Pagano RE. Transbilayer movement of fluorescent analogs of phosphatidylserine and phopshatidylethanolamine at the plasma membrane of cultured cells. Evidence for a protein mediated and ATP dependent process(es). J Biol Chem. 1987; 262:5890. [PubMed: 3571240]
39. Adams CS, Shapiro IM. The fate of the terminally differentiated chondrocyte: evidence for microenvironmental regulation of chondrocyte apoptosis. Crit Rev Oral Biol Med. 2002; 13:465. [PubMed: 12499240]
40. Verhoven B, Schlegel R, Williamson P. Mechanisms of phosphatidylserine exposure, a phagocyte recognition signal, on apoptotic T lymphocytes. J Exp Med. 1995; 182:1597. [PubMed: 7595231]
41. Wolfs JLN, Comfurius P, Rasmussen JT, Keuren JFW, Lindhout T, Zwaal RFA, Bevers EM. Activated scramblase and inhibited amniophospholipid translocase cause phosphatidylserine exposure in a district platelet fraction. Cell Mol Life Sci. 2005; 62:1514. [PubMed: 15971000]
42. Mandal D, Moitra PK, Saha S, Basu J. Caspase 3 regulates phosphatidylserine externalization and phagocytosis of oxidatively stressed erythrocytes. FEBS Lett. 2002; 513:184. [PubMed: 11904147]
43. Tischler M, Hecht P, Williamson J. Determination of mitochondrial/cytosolic metabolite gradients in isolated rat liver cells by cell disruption. Arch Biochem Biophys. 1977; 181:278. [PubMed: 18107]
44. Malik P, Fisher TC, Barsky LL, Zeng L, Izadi P, Hiti AL, Weinberg KI, Coates TD, Meiselman HJ, Kohn DB. An in vitro model of human red blood cell production from hematopoietic progenitor cells. Blood. 1998; 91:2664. [PubMed: 9531574]
45. Boesze-Battaglia K, Dispoto J, Kahoe MA. Association of a photoreceptor-specific tetraspanin protein, ROM-1, with Triton X-100-resistant membrane rafts from rod outer segment disk membranes. J Biol Chem. 2002; 277:41843. [PubMed: 12196538]
46. Allain CC, Poon LS, Chan CS, Richmond W, Fu PC. Enzymatic determination of total serum cholesterol. Clin Chem. 1974; 20:470. [PubMed: 4818200]
47. Bartlett GR. Phosphorous assay in column chromatography. J Biol Chem. 1959; 234:466. [PubMed: 13641241]
48. Bligh EG, Dyer WJ. A rapid method of total lipid extraction and purification. Can J Med Sci. 1959; 8:911.
49. Boesze-Battaglia K, Fliesler SJ, Li J, Young JE, Yeagle PL. Retinal and retinol promote membrane fusion. Biochim Biophys Acta. 1992; 1111:256. [PubMed: 1420260]
50. Skipski V, Smolowe AF, Barclay M. Separation of neutral glycosphingolipids and sulfatides by thin-layer chromatography. J Lipid Res. 1967; 8:295. [PubMed: 6033595]
51. Kamiya N, Jikko A, Kimata K, Damsky C, Shimizu K, Watanabe H. Establishment of a novel chondrocytic cell line N1511 derived from p53- null mice. J Bone Mineral Res. 2002; 17:1832.
52. Osyczka AM, Diefenderfer DL, Bhargave G, Leboy PS. Different effects of BMP-2 on marrow stromal cells from human and rat bone. Cells Tissues Organs. 2004; 176:109. [PubMed: 14745240]
53. Osyczka AM, Leboy PS. Bone morphogenetic protein regulation of early osteoblast genes in human marrow stromal cells is mediated by extracellular signal-regulated kinase and phosphatidylinositol 3-kinase signaling. Endocrinology. 2005; 146:3428. [PubMed: 15905316]
54. Wolfs JL, Comfurius P, Rasmussen JT, Keuren JF, Lindhout T, Zwaal RF, Bevers EM. Activated scramblase and inhibited aminophospholipid translocase cause phosphatidylserine exposure in a distinct platelet fraction. Cell Mol Life Sci. 2005; 62:1514. [PubMed: 15971000]
55. Williamson P, Christie A, Kohlin T, Schlegel RA, Comfurius P, Harmsma M, Zwaal RF, Bevers EM. Phospholipid scramblase activation pathways in lymphocytes. Biochemistry. 2001; 40:8065. [PubMed: 11434775]
56. McIntyre JC, Sleight RG. Fluorescence assay for phospholipid membrane asymmetry. Biochemistry. 1991; 30:11819. [PubMed: 1751498]
57. Bodin S, Giuriato S, Ragab J, Humbel BM, Viala C, Vieu C, Chap H, Payrastre B. Production of phosphatidylinositol 3,4,5-triphosphate and phosphatidic acid in platelet rafts: Evidence for a critical role of cholesterol-enriched domains in human platelet activation. Biochemistry. 2001; 40:15290. [PubMed: 11735411]

58. Bodin S, Tronchere H, Payrastre B. Lipid rafts are critical membrane domains in blood platelet activation processes. Biochim Biophys Acta. 2003; 1610:247. [PubMed: 12648778]
59. Boesze-Battaglia K, Clayton ST, Schimmel RJ. Cholesterol redistribution within human platelet plasma membrane: Evidence for a stimulus-dependent event. Biochemistry. 1996; 35:6664. [PubMed: 8639616]
60. Fadok V, Savill J, Haslett C, Bratton D, Doherty D, Campbell P, Henson P. Different populations of macrophages use either the vitronectin receptor or the phosphatidylserine receptor to recognize and remove apoptotic cells. J Immunol. 1992; 149:4029. [PubMed: 1281199]
61. Nanjundan M, Sun J, Zhao J, Zhou Q, Sims P, Wiedmer T. Plasma membrane phospholipid scramblase 1 promotes EGF-dependent activation of c-Src through the epidermal growth factor. J Biol Chem. 2003; 278:37413. [PubMed: 12871937]
62. Sheets ED, Lee GM, Simson R, Jacobson K. Transient confinement of a glycosylphosphatidylinositol-anchored protein in the plasma membrane. Biochemistry. 1997; 36:12449. [PubMed: 9376349]
63. Sims PJ, Wiedmer T, Esmon CT, Weiss HJ, Shattil SJ. Assembly of the platelet prothrombinase complex is linked to vesiculation of the platelet plasma membrane. Studies in Scott syndrome: an isolated defect in platelet procoagulant activity. J Biol Chem. 1989; 264:17049. [PubMed: 2793843]
64. Sun J, Nanjundan M, Pike LJ, Wiedmer T, Sims P. Biochemistry. 2002; 41:6338. [PubMed: 12009895]
65. Rami A, Sims P, Botez G, Winckler J. Spatial resolution of phospholipid scramblase 1 (PLSCR1), caspase-3 activation and DNA-fragmentation in the human hippocampus after cerebral ischemia. Neurochem Int. 2003; 43:79. [PubMed: 12605885]
66. Christian AE, Haynes MP, Phillips MC, Rothblat GH. Use of cyclodextrins for manipulating cellular cholesterol content. J Lipid Res. 1997; 38:2264. [PubMed: 9392424]
67. Ben-Efraim I, Zhou Q, Wiedmer T, Gerace L, Sims PJ. Phospholipid scramblase 1 is imported into the nucleus by a receptor-mediated pathway and interacts with DNA. Biochemistry. 2004; 43:3518. [PubMed: 15035622]
68. Glimcher, MJ. Composition, structure, and organization of bone and other mineralized tissues and the mechanism of calcification. In: Greep, RO., editor. Handbook of Physiology: Endocrinology. American Physiological Society; Washington, DC: 1976. p. 25
69. Glimcher MJ. The nature of the mineral component of bone and the mechanism of calcification. Instruct Course Lect. 1987; 36:49.
70. Gousset K, Wolkers WF, Tsvetkova NM, Oliver AE, Field CL, Walker NJ, Crowe JH, Tablin F. Evidence for a physiological role for membrane rafts in human platelets. J Cell Phys. 2002; 190:117.
71. Wiedmer T, Zhou Q, Kwoh DY, Sims PJ. Identification of three new members of the phospholipid scramblase gene family. Biochim Biophys Acta. 2000; 1467:244. [PubMed: 10930526]
72. Zhou Q, Zhao J, Al-Zoghaibi F, Zhou A, Wiedmer T, Silverman RH, Sims PJ. Transcriptional control of the human plasma membrane phospholipid scramblase 1 gene is mediated by interferon-alpha. Blood. 2000; 95:2593. [PubMed: 10753839]
73. Zhou Q, Zhao J, Wiedmer T, Sims PJ. Normal hemostasis but defective hematopoietic response to growth factors in mice deficient in phospholipid scramblase 1. Blood. 2002; 99:4030. [PubMed: 12010804]
74. Frasch S, Henson P, Kailey J, Richter D, Janes M, Fadok V, Bratton D. Regulation of phospholipid scramblase activity during apoptosis and cell activation by protein kinase Cdelta. J Biol Chem. 2000; 275:23065. [PubMed: 10770950]
75. Kametaka S, Shibata M, Moroe K, Kanamori S, Ohsawa Y, Waguri S, Sims PJ, Emoto K, Umeda M, Uchiyama Y. Identification of phospholipid scramblase 1 as a novel interacting molecule with beta-secretase (beta site amyloid precursor protein (APP) cleaving enzyme (BACE)). J Biol Chem. 2003; 278:15239. [PubMed: 12586838]
76. Gong X, Li E, Klier G, Huang Q, Wu Y, Lei H, Kumar NM, Horwitz J, Gilula NB. Disruption of alpha3 connexin gene leads to proteolysis and cataractogenesis in mice. Cell. 1997; 91:833. [PubMed: 9413992]

77. Lucic D, Mollenhauer J, Kilpatrcik KE, Cole A. N-telopeptide of type II collagen interacts with annexin V on human chondrocytes. Connect Tissue Res. 2003; 44:225. [PubMed: 14660093]

78. Gillete J, Nielson-Preiss SM. The role of annexin 2 in osteoblastic mineralization. J Cell Sci. 2004; 117:441. [PubMed: 14679310]

79. Gillette JM, Globus R, Nielson-Preiss SM. Annexin-2 and lipid raft involvement in osteoblastic mineralization. ASMBR. 2003; (Suppl):SU198.

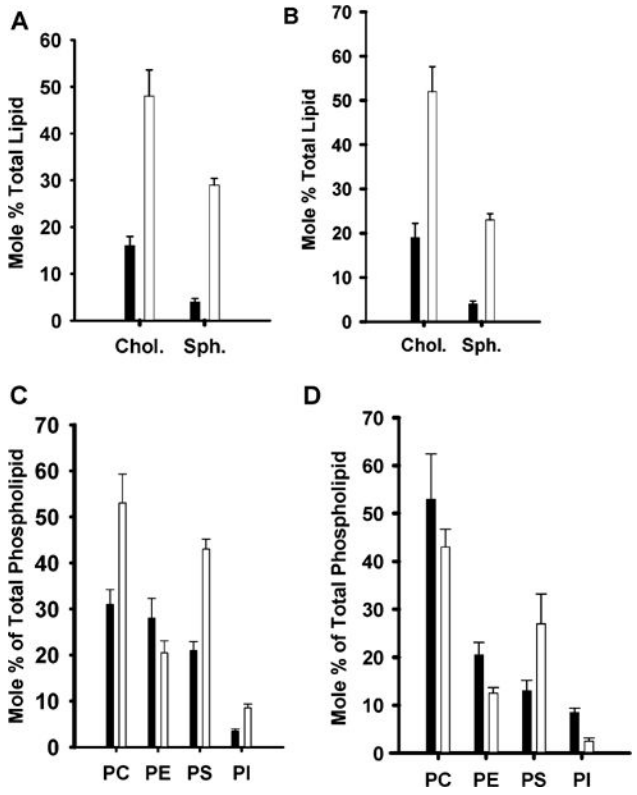

FIGURE 1.

Lipid profiles of chondrocyte and MV detergent resistant membranes. Cholesterol and sphingomyelin content of (A) chondrocyte membranes and (B) MV was determined as described in Materials and Methods in both detergent-soluble (solid black bars) and DRM fractions (white bars). Phospholipid profile of (C) chondrocyte membranes and (D) MV was determined as described in Materials and Methods in both detergent-soluble (solid black bars) and DRM fractions (white bars). Briefly, lipids were extracted from detergent-soluble and -insoluble fractions, the extract was dried down and resuspended, and phospholipids were separated using HPLC-ELSD or sequential 1D thin-layer chromatography (TLC) on silica gel G. All lipid analyses are an average of four individual analyses from three independent preparations.

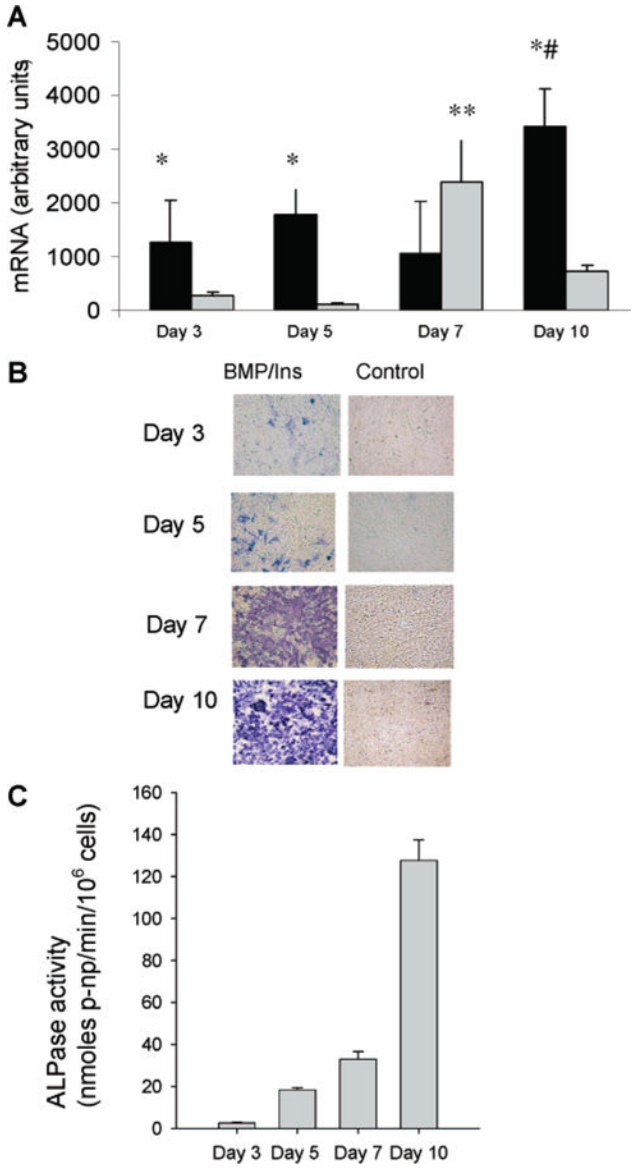

FIGURE 2.

Assessment of chondrocyte maturation. (A) Real-time RT-PCR of collagen X expression. N1511 cells were plated at a high density of 1.7×10^6 cells per well and induced with 50 ng/mL recombinant human BMP-2 and 1×10^{-6} M insulin (solid black bars). The cells in complete media constituted the control (solid gray bars). At the given time points RNA was extracted from cells and analyzed by real-time RT-PCR. The graph shows the mean values ± SD, expressed in mRNA arbitrary units. BMP/Ins-treated cells expressed higher levels of collagen X mRNA than corresponding controls as indicated by an * ($P < 0.001$ from the Tukey test). On day 10 collagen X expression in BMP/Ins-treated cells significantly increased as compared to days 3 and 7, as shown by a # ($P < 0.001$ from the Tukey test). Collagen X expression in control cells was the highest on day 7 as compared to days 3, 5, and 10 (**, $P < 0.001$ from the Tukey test). (B) Surface ALPase staining. Confluent N1511 cells were treated with BMP-2 and insulin, at the days indicated, and cells were

immunostained for ALPase surface expression as described in Materials and Methods. Representative data are shown from three different experiments with similar results. (C) ALPase activity in cultured chondrocytes. Confluent N1511 cells were treated with BMP-2 and insulin, at the days indicated, and ALPase activity was measured as described in Materials and Methods. The results are an average of three individual inductions, with ALPase activity measured in duplicate.

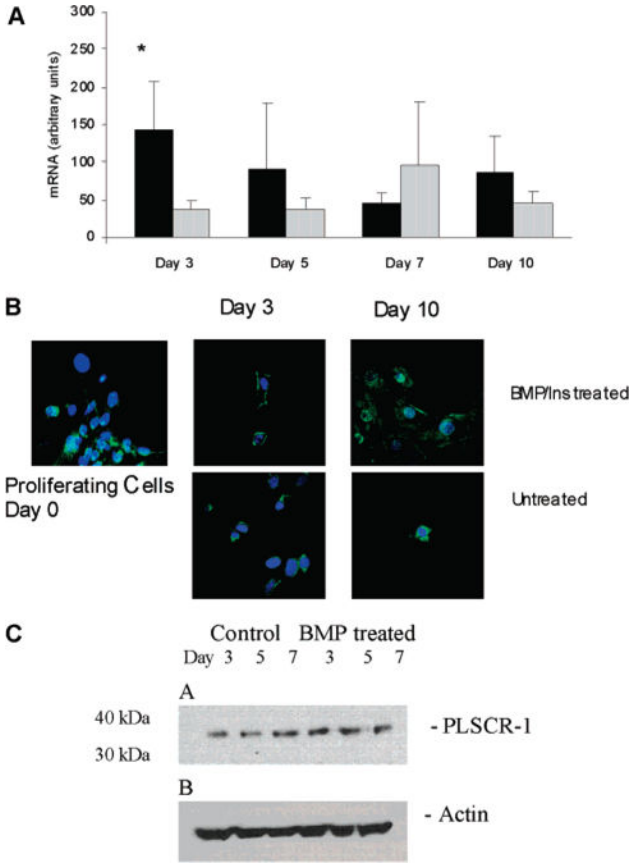

FIGURE 3.

Phospholipid PLSCR1 expression in N1511 cells during chondrocyte differentiation. (A) Real-time RT-PCR of PLSCR1 expression in N1511 cells. N1511 cells were plated at a high density. After 24 h (day 0) the cells were induced with 50 ng/mL recombinant human BMP-2 (R&D Systems), 1×10^{-6} M bovine insulin (Life Technologies, Inc.), and 50 μg/mL L-ascorbic acid phosphate (Wako) in media containing 0.3% FCS. The cells in complete media constituted the control. At the given time points RNA was extracted from cells and analyzed by real-time RT-PCR. The graph shows the mean values ± SD, expressed in mRNA arbitrary units. BMP/insulin-treated cells show higher levels of PLSCR1 expression than control cells as indicated by an *, with a $P < 0.05$ compared with corresponding untreated cells. (B) PLSCR1 localization in maturing chondrocytes. N1511 cells were treated with anti-PLSCR1 Ab-1 as described in Materials and Methods and assessed using laser confocal microscopy. (C) Expression of PLSCR1 protein in N1511 cells. Confluent N1511 cells were treated with BMP-2 and insulin, at the days indicated cells were isolated, and lysates were prepared in 35 mM OG. (A) The cell lysate was subjected to reducing electrophoresis, immunoblotted, and probed with 1 μg of anti-PLSCR1 antibody/mL of BLOTTO. (B) For actin protein loading controls, membrane was stripped and reprobed with a 1:250 dilution of anti-actin antibody (Santa Cruz Biotechnology).

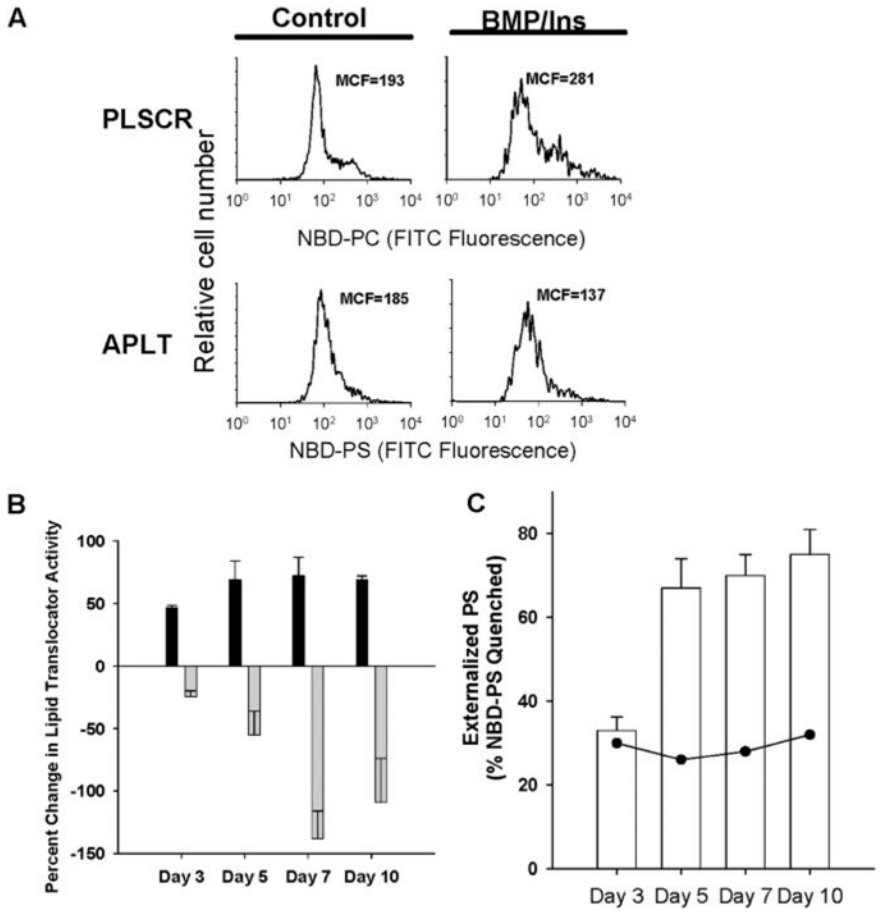

FIGURE 4.

Chondrocyte APLT and scramblase activities. N1511 cells isolated at the indicated times were labeled with either NBD-PS (APLT activity) or NBD-PC (scramblase), stained with propidium iodide, and analyzed for transporter activity by flow cytometry as described in Materials and Methods. (A) APLT and scramblase activity at day 5. Cytometry histograms are representative of data from three different experiments with similar results; 15000 cells were analyzed for each sample. (B) APLT and scramblase activity in maturing chondrcoytes. The percent change in mean channel fluorescence of NBD-PC, solid bars (scramblase activity), and NBD-PS, open bars (APLT activity), is indicated as chondrocytes mature. This percent change was calculated as the fluorescence change between BMP/Ins-treated and control cells as a function of BMP/Ins fluorescence for both APLT and scramblase activity. Mean fluorescence values were obtained by gating on viable (PI negative) cells. Routinely, cell viability was between 90% and 95%. (C) Externalization of PS in maturing chondrocytes. N1511 cells isolated at the indicated time points and labeled with acyl-chain-labeled NBD-PS were treated with 1 M sodium dithionite, and the change in fluorescence was recorded over 3 min. The solid line represents PS accessible to quenching in untreated control cells, and bars represent PS accessible to quenching in BMP/Ins-treated cells. The results are an average of three independent measurements of PS externalization. Error bars represent ±SD, with $n = 3$.

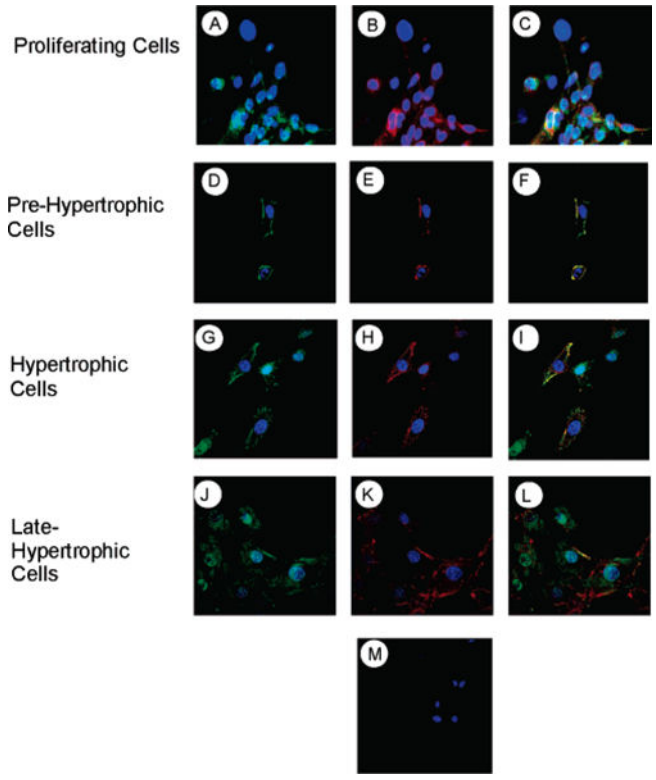

FIGURE 5.

Colocalization of PLSCR1 with GM1. N1511 cells were treated with CTb conjugated to AlexaFluor 594 and patched with anti-CTb antibody. The cells were then treated with anti-PLSCR1 Ab-1 as described in Materials and Methods and assessed using laser confocal microscopy. Images of AlexaFluor 488 fluorescence (panels A, D, G, and J) and AlexaFluor 594 fluorescence (panels B, E, H, and K) are shown as well as merged images (panels C, F, I, and L) showing both FITC (green) and AlexaFluor 594 (red) fluorescence along with DAPI stained. In controls, panel M, N1511 cells were treated with CTb and a 50:50 mix of AlexaFluor 488 and AlexaFluor 594 secondary antibodies and co-stained with DAPI. Results are representative of three experiments.

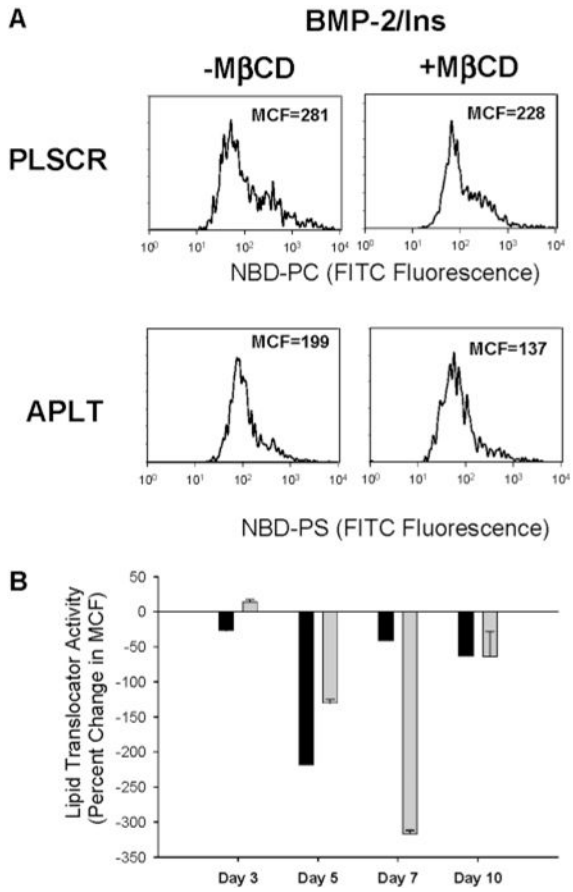

FIGURE 6.

Effect of MβCD on lipid translocator activity. N1511 cells isolated at the indicated times were labeled with either NBD-PS or NBD-PC to access APLT or scramblase activity, respectively. These cells were subsequently depleted of membrane cholesterol, with a short (10 min) incubation with 10 mM MβCD, stained with propidium iodide, and analyzed for transporter activity by flow cytometry as described in Materials and Methods. (A) Cytometry histograms are representative of data from three different experiments with similar results; 15000 cells were analyzed for each sample. (B) The percent change in mean channel fluorescence (MCF) values for scramblase activity (solid bars) and APLT activity (open bars) upon cholesterol depletion with MβCD is indicated. These mean fluorescence values were obtained by gating on viable (propidium iodide negative) cells. The cells used in these experiments are the same as those used in the studies shown in Figure 4 (activity prior to cholesterol depletion). Parallel experiments verified that MβCD did not adversely affect cell viability as determined by propidium iodide exclusion. Routinely, cell viability was approximately 90%. Data were analyzed using a one-way ANOVA analysis as described in Materials and Methods.

Table 1

Characteristics of Chondrocyte and Matrix Vesicle Detergent Resistant Membranes (DRMs)[a]

sample	% total phospholipid	Chol/Phos	% total GM1
chondrocytes		0.37–0.48	19.5 ± 2.4
chondrocyte rafts	6.9 ± 2.1	0.92–1.3	80 ± 4.9
MV		0.48–0.57	3.5 ± 1.2
MV rafts	32 ± 4.6	0.84–1.2	95 ± 7.8

[a] Chol/Phos refers to the cholesterol to phospholipid mole ratio of the various membrane fractions. Lipid phosphate and GM1 analyses represent the mean ± standard deviation of three independent preparations, each assayed in duplicate.

Table 2

Alkaline Phosphatase Activity of the Chondrocyte and MV Membrane Preparation[a]

sample	ALPase specific activity
purified chondrocyte membranes	0.58 ± 0.19
chondrocyte rafts	3.0 ± 1.2
purified MV	6.3 ± 1.5

[a]Alkaline phosphatase activity is expressed as millimoles of *p*-nitrophenyl phosphate per minute per milligram of protein and represents the mean ± standard deviation of four independent preparations, each assayed in duplicate.